Available online at www.sciencedirect.com
SCIENCE DIRECT®
Biochimica et Biophysica Acta 1655 (2004) 205–216
BIOCHIMICA ET BIOPHYSICA ACTA
BBA
www.bba-direct.com

Review

Tyrosyl radicals in Photosystem II

Idelisa Pujols-Ayala[1], Bridgette A. Barry*

Department of Biochemistry, Molecular Biology, and Biophysics, University of Minnesota, 1479 Gortner Ave., St. Paul, MN 55108, USA

Received 23 April 2003; received in revised form 31 July 2003; accepted 31 July 2003

Abstract

In PSII, there are two redox-active tyrosines, D and Z, with different midpoint potentials and different reduction kinetics. The factors responsible for these functional differences have not yet been elucidated. Recent model compound studies of tyrosinate and of tyrosine-containing dipeptides have demonstrated that perturbations of the amino and amide/imide group occur when the tyrosyl aromatic ring is oxidized [J. Am. Chem. Soc. 124 (2002) 5496]. Accompanying density functional calculations suggested that this perturbation is due to spin density delocalization from the aromatic ring onto the amino nitrogen. The implication of this finding is that spin density delocalization may occur in redox-active, tyrosine-containing enzymes, like Photosystem II. In this paper, we review the supporting evidence for the hypothesis that tyrosyl radical spin density delocalizes into the peptide bond in a conformationally sensitive, sequence-dependent manner. Our experimental measurements on tyrosyl radicals in dipeptides have suggested that the magnitude of the putative spin migration may be sequence-dependent. Vibrational spectroscopic studies on the tyrosyl radicals in Photosystem II, which are consistent with spin migration, are reviewed. Migration of the unpaired spin may provide a mechanism for control of the direction and possibly the rate of electron transfer.

Keywords: Redox active; Electron transfer; EPR; FT-IR; Photosynthetic water oxidation; Isotope labeling

1. Introduction

Redox-active tyrosine residues (Fig. 1) play important roles in catalysis in several enzymes, including ribonucleotide reductase, prostaglandin H synthase, and Photosystem II. In these enzymes, tyrosyl radicals are proposed to act as intermediaries in long-distance electron transfer reactions. Environmental factors can play important roles in controlling the role of the redox-active tyrosine in catalysis. This is particularly clear in the case of Photosystem II, which contains two unmodified, redox-active tyrosines. These two tyrosines, D and Z, have different reduction kinetics and different midpoint potentials (see discussion below). The environmental interactions that control the midpoint potential and the electron transfer properties of these redox-active tyrosines are still unknown. In an effort to understand the biological function of tyrosyl radicals, we have performed model compound studies, in which the functional differences imposed by peptide bond formation and peptide sequence have been investigated.

2. Overview of electron transfer in Photosystem II

The primary chl donor of PSII is called P_{680}. After light absorption, P_{680} transfers an electron from an excited electronic state to a nearby pheophytin (Pheo), which in turn reduces a bound plastoquinone, called Q_A (Fig. 2). Q_A reduces a second quinone, Q_B. Unlike Q_A, which is a single electron acceptor, Q_B is a two-electron acceptor. The fully reduced quinol form of Q_B, Q_BH_2, acts as a diffusible electron carrier in the membrane. On the donor side of PSII, P_{680}^+ oxidizes a tyrosine residue, Z, which in turn oxidizes the catalytic site of water oxidation. The catalytic site contains four manganese atoms, in addition to calcium and chloride ions. The release of oxygen requires four sequential charge separations and oxidations; the catalytic

Abbreviations: chl, chlorophyll; D, tyrosine 160 of the D2 polypeptide of PSII; EPR, electron paramagnetic resonance spectroscopy; FT-IR, Fourier transform infrared spectroscopy; PSII, Photosystem II; Z, tyrosine 161 of the D1 polypeptide of PSII

* Corresponding author. Present address: School of Chemistry and Biochemistry, Georgia Institute of Technology, Atlanta, GA 30332, USA. Tel.: +1-404-385-6085; fax: +1-404-894-2295.
E-mail address: bridgette.barry@chemistry.gatech.edu (B.A. Barry).
[1] Present address: Broward Community College, 3501 SW Davie Rd., Davie, FL 33314, USA.

0005-2728/$ - see front matter © 2004 Elsevier B.V. All rights reserved.
doi:10.1016/j.bbabio.2003.07.010

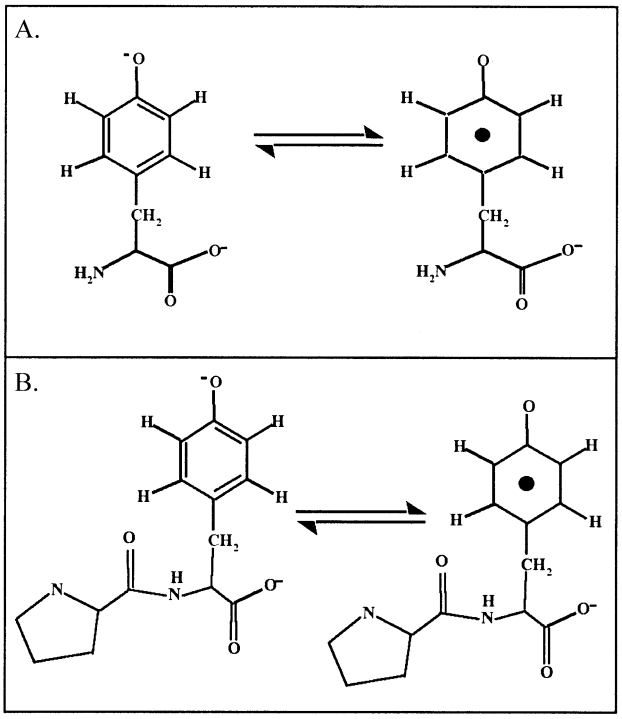

Fig. 1. One electron oxidation to form a neutral tyrosine radical in tyrosinate (A) and in the tyrosinate-containing dipeptide, pro–tyr (B).

site can accumulate the four oxidizing equivalents necessary to generate oxygen from water. The sequentially oxidized forms of the catalytic site are called the S_n states, where *n* refers to the number of oxidizing equivalents stored at the active site (reviewed in Ref. [1]). Redox-active tyrosine D is an additional redox-active component in PSII. Tyrosine D may play a role in photoassembly of the catalytic site [2].

An oxygen-evolving PSII preparation is composed of multiple subunits. Both intrinsic and extrinsic subunits are present. CP47 and CP43 are intrinsic, chlorophyll-binding proteins. The Mn-stabilizing protein (MSP or 33 kDa protein), the 24-kDa proteins, and the 18-kDa proteins are extrinsic subunits that modulate the properties of the catalytic site in plants. The 18- and 24-kDa subunits are not present in cyanobacteria (reviewed in Ref. [3]). Two of the hydrophobic PSII subunits, called D1 and D2, bind most of the prosthetic groups that are involved in electron transfer. These subunits form the heterodimer core of the PSII reaction center [4]. Recently, 3.7 and 3.8 Å structures of cyanobacterial PSII have been reported [5,6]. These structures are not yet at high enough resolution to resolve amino acid side chains or to define all of the subunits.

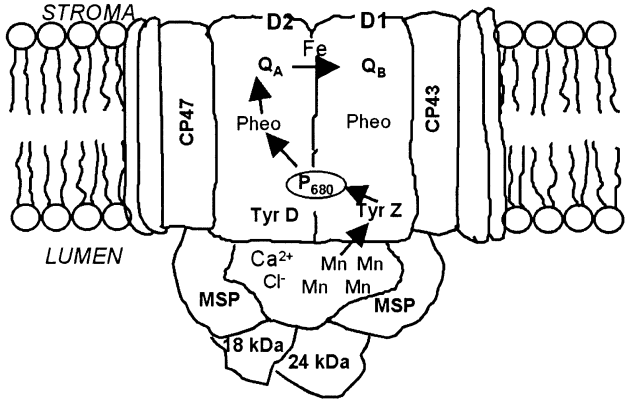

Fig. 2. Schematic of PSII structure.

3. Tyrosyl radicals in Photosystem II

As mentioned above, PSII contains two well-characterized redox-active tyrosine residues, D and Z, with characteristic EPR spectra in the oxidized state (Fig. 3A). Redox-active tyrosine Z conducts electrons between P_{680} and the manganese cluster and is required for oxygen evolution [7]. Redox-active tyrosine D forms a stable neutral radical (Fig. 3A, dashed line) and is not required for steady state oxygen evolution [8,9]. Site-directed mutagenesis shows that tyrosine Z is tyrosine 161 of the D1 polypeptide and that tyrosine D is tyrosine 160 of the D2 polypeptide [8–12]. These redox-active tyrosines are therefore predicted to be in C_2 symmetrically related positions in the D1 and D2 subunits. However, as described above, only one of the two side chains is involved in the electron transfer events that lead to water oxidation. Such structural symmetry, but functional asymmetry, is also observed in the arrangement of the bacteriopheophytin acceptors in the bacterial reaction center [13].

The tyrosyl radicals in PSII have different midpoint potentials [11,14]. The rates at which D^{ox} and Z^{ox} are reduced also differ by orders of magnitude. In oxygen-evolving samples, Z^{ox} is reduced by the manganese-containing catalytic site in the microsecond–millisecond time scale [7,15]. As shown by Babcock et al. [16], the rate of reduction depends on the S state. In samples from which the manganese is removed, the EPR lifetime of Z^{ox} increases to the millisecond time scale [17]. Under illumination, an EPR signal from Z^{ox} is generated in these PSII preparations (Fig. 3). In the dark, Z^{ox} is reduced by exogenous and endogenous donors (see Ref. [18] for a

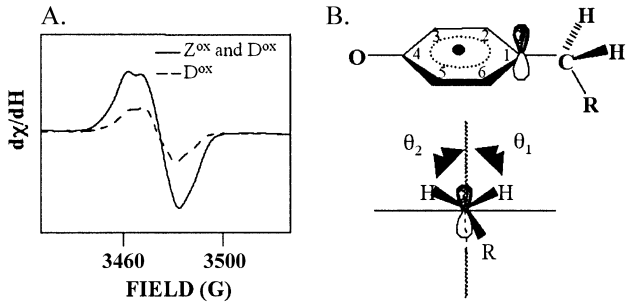

Fig. 3. (A) EPR spectra of D^{ox} and Z^{ox}. (B) Numbering for tyrosyl radical and definition of methylene angles. The angles θ_1 and θ_2 are not necessarily equal.

recent example). On the other hand, D^{ox} is stable in the dark for minutes to hours, depending on the PSII preparation (for example, see Ref. [19]). There is one spin of D^{ox} per reaction center, and up to one spin of Z^{ox} can be generated (reviewed in Ref. [20]). For both signals, the *g* value is 2.004, the width is ~ 20 G, and partially resolved hyperfine splittings are observed (Fig. 3A).

Because D and Z are both tyrosine residues with different functions, each tyrosine must have a different interaction with its environment. Although the EPR signals of D^{ox} and Z^{ox} are similar, magnetic resonance techniques can detect small differences in the distribution of conformations at the methylene carbon (Fig. 3B) (for examples, see Refs. [21–24]). Changes in the conformation at the methylene carbon alter the EPR spectrum by changing hyperfine couplings to the β-protons (Fig. 3B). However, these data suggest only subtle differences in structure at the C_1-C_β single bond, when D^{ox} and Z^{ox} are compared.

One possible modulator of D and Z midpoint potential is the polarity of their environments [25]. A potential, additional modulator of Z and D redox potential is the identity of the proton acceptor. The *g* values of Z^{ox} and D^{ox} predict that both residues are deprotonated when oxidized [21,26]. D and Z may be either tyrosinate or tyrosine in the ground state and, therefore, proton transfer may be coupled to the electron transfer reaction. With just a few exceptions, the majority of the literature supports the conclusion that, for both Z and D, proton transfer accompanies electron transfer, indicating that tyrosine Z and D are neutral in the ground state (see Refs. [27,28] and references therein). However, changes in pH have been reported to have differential effects on the oxidation kinetics of tyrosine D and Z [29,30]. This result suggests that, while proton transfer accompanies the redox reactions of both D and Z, the mechanism of proton transfer distinguishes the redox-active tyrosines.

When proton transfer accompanies electron transfer, alterations in the pK_a of the proton acceptor(s) can have an important impact on the midpoint potential. Early models of PSII, based on the nonwater splitting bacterial reaction center, had originally suggested that a histidine is in close proximity to each redox-active tyrosine, with His-189-D2 predicted to be in close proximity to tyrosine D and with His-190-D1 predicted to be in close proximity to tyrosine Z [31,32].

The role of histidine 189 of the D2 polypeptide was investigated in our laboratory through the use of reaction-induced FT-IR spectroscopy [27]. Magnetic resonance experiments had shown that histidine 189 is hydrogen bonded to D^{ox} [33–36]. However, magnetic resonance techniques observe only the paramagnetic state and cannot give information about structural changes, linked to electron transfer reactions, in PSII. A valuable aspect of difference FT-IR spectroscopy is that structural changes in the environment of redox-active tyrosines will also be observed. In this technique, light and dark spectra are subtracted, to give the difference spectrum associated with D^{ox} reduction. To test whether histidine 189 is a proton acceptor for tyrosine D, FT-IR spectroscopy, isotopic labeling, site-directed mutagenesis of His-189-D2, and chemical complementation were combined [27]. This work showed that His-189-D2 is involved in a reversible protonation reaction, when the tyrosyl radical D^{ox} is reduced. In this study, efficient proton transfer was found to be a requirement for efficient D^{ox} electron transfer [27].

EPR and FT-IR spectroscopy were used to investigate the role of His-190 in the D1 polypeptide. Early work had suggested that His-190 is not the proton acceptor for tyrosine Z [37,38]. Recently, our laboratory has provided additional evidence supporting that conclusion [18]. While a glutamine mutation at His-190 had deleterious effects on Z electron transfer reactions at room temperature, at lower temperatures, these deleterious effects were dramatically reduced in magnitude. These results suggest that the glutamine substitution at His-190 causes a temperature-dependent structural destabilization of PSII [18]. This structural destabilization may be responsible for some or all of the phenotypic changes documented in this mutant [39,40]. This conclusion is supported by preliminary conclusions from recent low resolution PSII X-ray structures, which both suggest that His-190 and tyrosine Z are not in close proximity [6,41], but see [77].

4. Labeling and the EPR identification of D^{ox} and Z^{ox}, plastoquinone or tyrosine?

In the 1980s, Babcock et al. suggested that a likely origin of the D^{ox} EPR signal was plastoquinone, which was bound on the donor side of PSII and was oxidized by the primary chlorophyll donor, P_{680}^{+}, to give a plastoquinone cation radical [42]. To test this idea, Barry and Babcock [26] deuterated plastoquinone by growth of a cyanobacterial methionine auxotroph on $^2H_3$-labeled methionine. When no change in the D^{ox} EPR signal was observed, a tyrosine origin for the signal was tested. Tyrosine was deuterated by growth of cyanobacteria under conditions in which the organism was a functional auxotroph for tyrosine. This was accomplished by growth of cultures in the presence of all three aromatic amino acids: tyrosine, tryptophan, and phenylalanine. Deuteration of tyrosine resulted in narrowing of the D^{ox} EPR signal and provided support for a tyrosyl radical assignment of the D^{ox} signal [26]. Further experiments, in which tyrosine was specifically deuterated, showed that the aromatic ring of D^{ox} was not covalently modified with another amino acid and that the expected odd alternate pattern of spin density was observed [43]. These experiments were performed using intact cyanobacterial cells. After the development of PSII purification method from this organism [44], a tyrosine origin for Z^{ox} was demonstrated by Boerner and Barry [21] through specific deuteration.

5. FT-IR band assignments in Photosystem II, tyrosine or plastoquinone?

As stated above, FT-IR spectroscopy has the potential to reveal information about the interactions of redox components with the protein environment. The expected tyrosine-based oxidation changes are perturbations to the ring stretching (υ8a, υ19a) and CO stretching (υ7a) vibrations, as unpaired spin density delocalizes to the phenol oxygen [45,46]. Other spectral contributors arise from redox-linked and protonation changes in the environment, as described above. In our work, isotopic labeling, EPR, fluorescence, and kinetic FT-IR experiments of tyrosine were used to assign vibrational lines to redox-active tyrosines [19,47–50]. When alternative spectral assignments were proposed [51–53], additional experiments were performed to evaluate that interpretation [54,55]. This project, in which tyrosyl radical and plastoquinone anion radical vibrational bands must be distinguished, is described below.

6. FT-IR studies on the plastoquinone acceptors in PSII

In 1990, Berthiomeiu et al. [56] assigned a light-induced FT-IR spectrum to Q_A reduction in PSII. The spectrum was acquired in the presence of the electron donor and PSII inhibitor, hydroxylamine. A band at 1478 cm^{-1} was assigned to the CO vibration of Q_A^-. In 1997, time-resolved FT-IR experiments confirmed that a band at 1478 cm^{-1} decayed with kinetics that were consistent with the decay of Q_A^- [57]. Similar assignments for Q_B^- have been proposed [58]. In 1999, a plastoquinone methyl labeling experiment was reported by Razeghifard et al. [49], and this experiment supported the assignment of a band at 1480 cm^{-1} to Q_A^-. Data were collected under cryogenic conditions (80 K), where Q_A^- can be generated quantitatively by illumination. At the available spectral resolution of the experiments, this 1480 cm^{-1} contributor from Q_A^- may be equivalent to the 1478 cm^{-1} spectral component, observed in the kinetic experiments [57]. Accompanying density functional calculations suggested a ring CC antisymmetric stretching vibration assignment for the 1480 cm^{-1} band [49], not a CO assignment. Thus several lines of evidence are consistent with a Q_A^- contribution at 1480 cm^{-1}.

However, in Ref. [49] the spectrum associated with plastoquinone reduction in vitro was reported. This in vitro reduction spectrum is different from the spectrum assigned to a pure Q_A^- spectrum in Ref. [56]. In particular, the relative intensities of bands in the 1650–1630 and 1480–1460 cm^{-1} regions differ when the model compound and PSII spectra are compared. As noted [59] in the presence of hydroxylamine, oxidation of tyrosine D and chl $_Z$ may be observed in PSII. Chl Z [59,60] and tyrosine D (see discussion below) have overlapping spectral contributions in the 1480 cm^{-1} region. The chl $_Z$ contribution is ^{15}N sensitive and can be distinguished on this basis [59]. This is a region in which strong IR absorption from CH bending and CC stretching vibrations is expected, so it is not surprising that there can be overlapping contributions from multiple PSII species Q_A^-, D, chl, in this region.

7. Redox-active tyrosines in PSII have a spectral contribution at 1478 cm^{-1}

In Fig. 4A, we present a difference FT-IR spectrum, which has an intense band at 1478 cm^{-1}. The evidence that this spectrum arises from tyrosine Z oxidation and not from Q_A reduction is reviewed here. In particular, a combination of kinetic and isotopic labeling work has shown that a component of the 1478 cm^{-1} band is assignable to the CO stretch (υ7a) of Z^{ox}.

7.1. Overview

In early work, the FT-IR spectrum, assigned to Z^{ox}-minus-Z, was acquired under conditions in which an EPR signal from tyrosyl radical Z^{ox} was observed [19,47,61]. This spectrum was observed in cyanobacterial PSII under conditions in which Q_A^- contributions were determined to be negligible [19,48]. Site-directed mutants, generated on the donor side of PSII, were observed to alter the spectrum [18]. Finally, the PSII inhibitor, hydroxylamine, which blocks formation of Z^{ox} [62], changes the spectrum [19,48]. Taken together, these experiments support a Z^{ox} assignment.

7.2. Kinetic experiments

Kinetics are a valuable tool in making spectral assignments when there are overlapping spectral contributions, as in the case of the 1478 cm^{-1} region. In published work [55], the decay kinetics of Q_A^- and Z^{ox} were monitored with chl fluorescence and EPR spectroscopy, respectively. Cyanobacterial manganese-depleted PSII was employed, in which Z is the terminal electron donor and Q_A is the terminal electron acceptor. Potassium ferricyanide and ferrocyanide were present as exogenous electron acceptor and donor, respectively. The decay of Q_A^- was monoexponential and gave an overall rate constant of 3.2 s^{-1} [55]. The decay of Z^{ox} (Fig. 4H) was observed to be biexponential. To explain these kinetic data, we proposed a model in which Z^{ox} and Q_A^- recombine with a rate constant of 1.8 s^{-1} in 60% of the centers [55]. In the other 40%, Q_A^- is oxidized by potassium ferricyanide with a time constant of 1.4 s^{-1}, and Z^{ox} is reduced slowly by ferrocyanide (rate constant, 0.2 s^{-1}). A critical point is that there is a slow phase in Z^{ox} decay, which is clearly distinguishable (factor of 16) from the decay of Q_A^-.

FT-IR spectroscopy was then used to follow the decay of the 1478 cm^{-1} band (Fig. 4A–E). With the available time resolution (1.3 s per spectra), fast-decaying components,

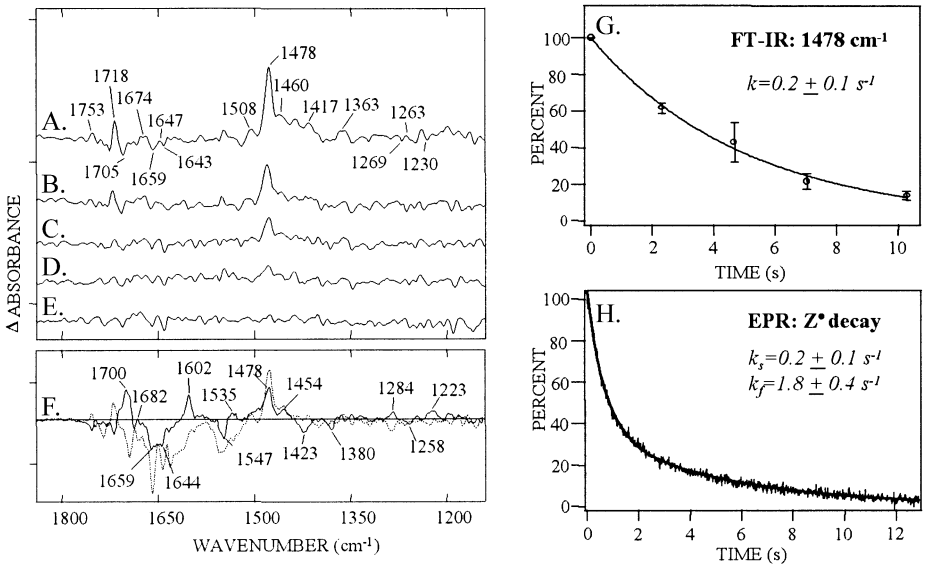

Fig. 4. Difference FT-IR spectra of $Z^{ox}-Z$ in spinach PSII, showing the decay of the signal (A–E). Effects of $^{13}C_6$ (ring) tyrosine labeling on the FT-IR spectrum, associated with the oxidation of tyrosine Z in manganese-depleted cyanobacterial PSII (F). Time dependence of Z^{ox} decay as assessed by FT-IR (G) and EPR (H) measurements in manganese-depleted spinach PSII. Spectra were recorded in 1.3 s, according to the conditions described in Ref. [55]. (Figure reprinted with permission from *Biophysical Journal*.)

originating from recombination of Z^{ox} and Q_A^- and the oxidation of Q_A^- by ferricyanide, will not be observed. Fits to the FT-IR kinetics (Fig. 4G) indicated that a slow decaying component of the 1478 cm^{-1} band has a 0.2 s^{-1} rate constant [55]. This rate constant matches the slow phase observed in the EPR-derived decay of Z^{ox}, but is clearly distinguishable from the 16-fold faster rate of Q_A^- decay. Therefore, this kinetic experiment supports a Z^{ox} assignment for a component of the 1478 cm^{-1} band.

7.3. [^{13}C]tyrosine labeling

Another experiment supporting the Z^{ox} assignment was performed by labeling tyrosine with ^{13}C. Labeling the tyrosine ring at all six positions ($^{13}C_6$) or at one ($^{13}C_1$) position caused a downshift of a component of the 1478 cm^{-1} band [19,48,55]. This is illustrated in Fig. 4F for the $^{13}C_6$ labeling case. Fig. 4F (solid line) is the isotope-edited, double-difference spectrum. To construct this isotope-edited spectrum, the Z^{ox}-minus-Z spectrum, acquired with the ^{13}C isotopomer, was subtracted from the natural abundance control data. The spectrum of the natural abundance ^{12}C control is shown superimposed as a dashed line on the isotope-edited data (Fig. 4F, solid line). Isotope shifts of bands in the 1800–1200 cm^{-1} region are observed in the double-difference spectrum. In particular, a component of the 1478 cm^{-1} band, which is positive in the isotope-edited spectrum, shifts to 1423 cm^{-1}, becoming negative (Fig. 4F, solid line). The entire 1478 cm^{-1} band does not shift, however. Remaining, nonisotope sensitive intensity was assigned to Chl, due to observed ^{15}N sensitivity [38,59]. When tyrosine was ^{13}C labeled at the carbon bound to the phenol oxygen, a $^{13}C_1$ induced downshift (to 1469 cm^{-1}) was also observed [50]. Additional isotopic shifts were observed in the ring stretching region of this spectrum (1600–1500 cm^{-1}), which could be due to the expected isotope sensitive in the ring stretching vibrations. However, the rest of the spectrum was not assigned, due to the possibility of baseline difficulties in the amide I and II region, which can distort frequencies in the double-difference spectrum. To summarize, a component of the 1478 cm^{-1} band downshifts in samples in which tyrosine is either $^{13}C_6$ or $^{13}C_1$ ring labeled.

7.4. [^{2}H]plastoquinone labeling

As stated above, control experiments indicated that under the conditions used to acquire the Z^{ox}-minus-Z spectrum (−10 °C) in cyanobacteria, there is a low steady state concentration of Q_A^-. To test this conclusion, we investigated the effect of ^2H plastoquinone labeling under these conditions [50]. If Z oxidation dominates the FT-IR spectrum, then the effects of plastoquinone labeling on the spectrum should be minimal. If Q_A reduction dominates the FT-IR spectrum, then the isotope effects will resemble those recorded at 80 K [49]. Mass spectrometric analysis was used to show that tyrosine is not labeled under the conditions used for ^2H quimone labeling [50]. With plastoquinone labeling, the spectral results showed only a minor change in the amplitude of the 1478 cm^{-1} line. The changes induced by tyrosine labeling were more dramatic. The small spectral change observed with plastoquinone deuteration allowed an estimate of the amount of Q_A^- contributing to the spectrum under these conditions. This was performed through a comparison with isotope-edited spectra acquired at 80 K, where Q_A^- is produced in maximum yield. The

results indicated that only 10% of the centers produced a stable Q_A^- under the conditions employed to measure the Z^{ox}-minus-Z spectrum in cyanobacterial PSII. This low level of Q_A^- is consistent with earlier EPR and fluorescence controls (see discussion above), and is another indication that this −10 °C spectrum is dominated by oxidation of the redox-active tyrosine residue.

7.5. [$2H_4$]tyrosine labeling

In the course of this ^{13}C-labeling work, mass spectrometric analysis revealed that ^{13}C label from the tyrosine ring is incorporated into plastoquinone [50]. Although the amount of this label scrambling was at relatively low levels (~20% for the $^{13}C_1$ isotopomer and 60% for the $^{13}C_6$ isotopomer) and Q_A^- contributions to the data were also determined to be small (<10%) [50], isotope labeling under conditions in which plastoquinone is not significantly labeled is clearly advantageous. In addition, an improvement in spectral baseline and signal-to-noise would allow the assignment of the entire 1800–1200 cm^{-1} region. Therefore, tyrosine was d_4 ring labeled in PSII, and FT-IR spectra were acquired [63]. Early [26] and recent [50] mass spectrometry experiments showed that no significant ^2H label was incorporated into plastoquinone from tyrosine. The PSII data (Fig. 5D–F) were compared to model compound data obtained from d_4-labeled tyrosinate (Fig. 5A–C). Comparison of the two data sets shows that the double-difference, isotope-edited spectra (natural abundance-minus-$^2H_4$ labeled tyrosine) exhibit multiple bands that are similar in frequency and relative amplitude.

For example, ring stretching vibrations, observed in the PSII spectrum (Fig. 5F), resemble ring stretching vibrations observed in the model compound (Fig. 5C). In the PSII data (Fig. 5F), bands at (−) 1602 and (+) 1583 cm^{-1} were assigned to υ8a of Z and its isotopomer, respectively. Bands at (+) 1558 and (−) 1547 cm^{-1} were assigned to υ8a of Z^{ox} and its isotopomer, respectively [63]. These frequencies are within 5–20 cm^{-1} of the observed frequencies of these bands in model tyrosinate and tyrosyl radical (Fig. 5C). A positive 1421 cm^{-1} band in Fig. 5F was assigned to the isotopically shifted υ19a band, which is the most intense spectral feature in the in vitro data (Fig. 5C). In the Z^{ox} minus-Z spectrum, υ19a of the unlabeled Z species was tentatively assigned to a negative spectral feature at 1531 cm^{-1}. In Fig. 5F, a (+) 1480/(−) 1471 cm^{-1} derivative-shaped feature was assigned to the CO stretching vibration, υ7a, which is downshifted (37–28 cm^{-1}) from the observed (+) 1517/(−) 1499 cm^{-1} frequencies in the model compound (Fig. 5C). Notice that the magnitude of the $^2H_4$ isotope effect for this band is one half the isotope effect observed for υ7a in model tyrosyl radical (Fig. 5C). This may be due to decreased coupling between CO and ring vibrational modes caused by the decrease in frequency. The downshift of Z^{ox} CO frequency was attributed [63] to delocalization of spin density from the phenol oxygen to the amide/imide bonds (see below). In Fig. 5F, there were no intense bands observed at (−) 1258 and (+) 1234 cm^{-1}. In

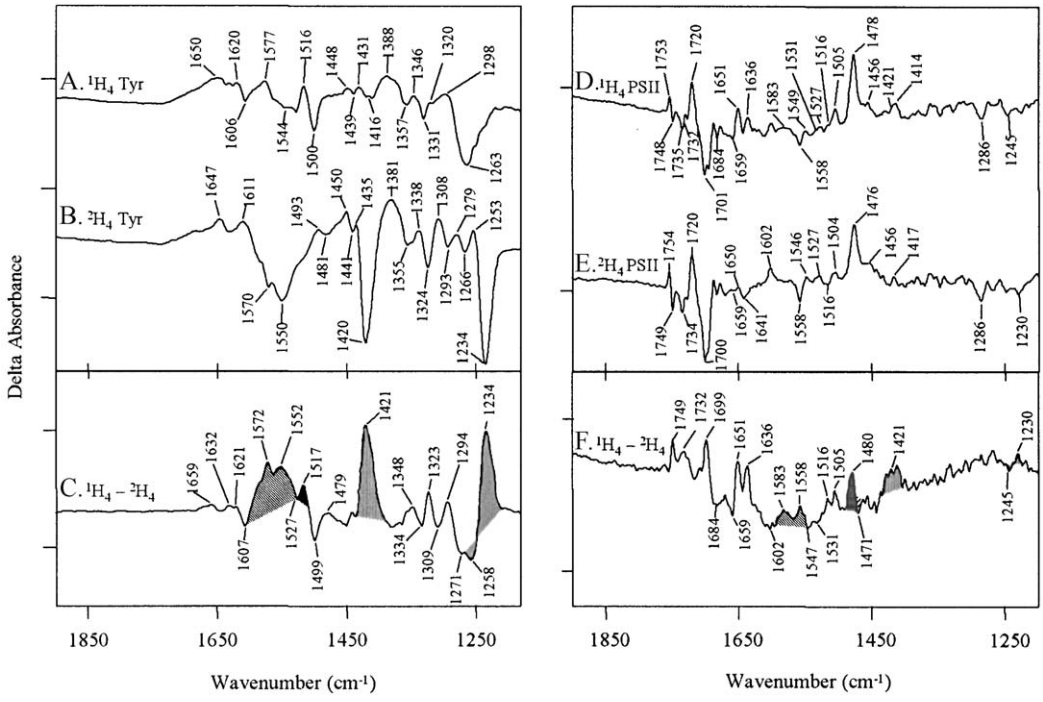

Fig. 5. Difference FT-IR spectra associated with the oxidation of tyrosinate at 77 K (A–C) and of tyrosine Z in photosystem II at 263 K (D–F). In A and B, spectra were acquired on natural abundance tyrosinate and $^2H_4$-ring-labeled tyrosinate, respectively, in 10 mM borate–NaOH, pH 11. C shows the isotope-edited spectrum (A–B). In D and E, spectra were acquired on natural abundance Z and $^2H_4$-ring labeled Z, respectively. F shows the isotope-edited spectrum (D–E). See Ref [63] for experimental details. (Figure reprinted with permission from Ref. [63]. Copyright (2003) *Journal of the American Chemical Society*.)

the model compound (Fig. 5C), these spectral features arise from the CO stretching vibration (υ7a′) of tyrosinate and its isotopomer. In the PSII data (Fig. 5F), weak bands at (−) 1245 and (+) 1230 cm^{-1} may correspond to υ7a′ of Z and its isotopomer, but the signal-to-noise was not sufficient to assign these bands with confidence [63]. Therefore, we concluded that the amplitude and, possibly, frequency, of υ7a′ is perturbed, when Z is compared to the model tyrosinate compound. This result is consistent with a protonated, hydrogen-bonded state for Z; in such a state, the intensity of the CO band is known to be small [63,64]. Contributions to the in vivo isotope-edited spectrum (Fig. 5F) at ∼1700 cm^{-1} were attributed to a small amount of incorporation of label into glutamic acid [63]. Glutamic acid does not make any additional contribution to the spectral region between 1605 and 1230 cm^{-1} [65].

The FT-IR spectrum, associated with tyrosine D oxidation, has also been reported [19,27,38,47,48,54]. Tyrosine D can be distinguished from tyrosine Z on the basis of its slow decay kinetics [47]. While the spectra of tyrosine D and Z have 1478 cm^{-1} bands, the spectra are not identical. See Ref. [54] for a discussion of this point.

8. Alternant assignments for tyrosine Z and D

Alternant assignments for tyrosine D and Z, which do not involve a spectral contribution at 1478 cm^{-1}, have been presented [51–53]. Bands were assigned to a CO vibration of D^{ox} (1503 cm^{-1}) and Z^{ox} (1512 cm^{-1}) based on isotopic labeling of tyrosine. Bands at 1275 and 1279 cm^{-1} were assigned to the CO stretching vibration of D and Z.

To discuss these alternant tyrosine Z assignments, one concern is the choice of a time regime for data acquisition. A time regime was chosen in which the majority of Z (80–85%) had already decayed, as assessed by optical techniques [53]. No 1478 cm^{-1} band was observed under these conditions, but this might be expected, because the concentration of Z^{ox} was low [55].

In addition, no mass spectrometry experiments were performed to track label scrambling, and the putative isotope effects observed in those data are not easily rationalized and do not closely resemble the isotope shifts observed for tyrosine model compounds [63,66–68]. In difference spectra acquired from model compounds, the CO stretching vibration (υ7a) and ring stretching vibrations (υ8a and υ19a) have similar intensities, and labeling of the ring either with ^{13}C or $^{2}H_4$ causes isotope shifts in observed ring and CO vibrational bands (see Refs. [63,66–68] and Fig. 5C). However, in Ref. [53], isotope shifts were not observed for all bands. To give examples, there was no shift of bands, assignable to υ8a of Z and Z^{ox}, in the $^{13}C_1$ tyrosine-labeled sample, and there was no shift of Z υ19a in the $^{13}C_1$ or $^{13}C_6$ sample (see Table 1 in Ref. [53]). To give another example, while a shift of a putative CO vibration (1512 cm^{-1}) was observed when tyrosine was $^{13}C_1$ labeled, there was no clear evidence for a 1512 cm^{-1} band shift when tyrosine was $^{13}C_6$ labeled or $^{2}H_4$ labeled (but see Table 1 in Ref. [53]). In addition, upon $^{2}H_4$ labeling, the most intense band in the difference spectrum should be the isotopically shifted υ19a ring vibration of Z (see Fig. 5C,F for an example). However, this band was not observed in Ref. [53]. Taken together, these results might be most consistent with label scrambling. Another point to consider is that kinetics were never used to track the amplitude of the 1512 cm^{-1} band and to correlate band amplitude changes with Z^{ox} decay, as assessed by another technique.

Issues, concerning the use of phosphate/formate in the samples used for the tyrosine D assignments, have been raised [54]. In addition, many of the points raised above apply to the alternant tyrosine D assignment as well as to the tyrosine Z assignment.

9. Oxidation of tyrosinate in vitro

One interesting point to arise from our FT-IR work is that the bands assigned to the CO vibrations of D^{ox} and Z^{ox} [19,27,47,48,50,55,63] are low in frequency (1478 cm^{-1}) compared to the CO vibration of tyrosyl radical (1516 cm^{-1}), produced from tyrosinate in vitro [68]. The CO vibration of the stable tyrosyl radical in ribonucleotide reductase is also low in frequency and has been assigned at 1498 cm^{-1} [69]. The explanation for these changes in frequency, observed in tyrosyl radicals in vivo, was investigated using model compound studies. Flash UV photolysis was used to oxidize the aromatic ring of tyrosinate at low temperature in polycrystalline powders (Fig. 1A). Photolysis generated a neutral tyrosyl radical, which gave rise to an EPR signal that resembles tyrosyl D^{ox} and Z^{ox} (Fig. 6A). The reaction was performed with specifically deuterated tyrosines [67,68], and simulations were performed to determine the magnitude of specific hyperfine couplings, as previously described [67,68,70]. Large hyperfine couplings were observed to the 3 and 5 protons as well as to one of two methylene protons. This result is consistent with significant spin densities at the 1, 3, and 5 ring positions. Fig. 6B shows the EPR spectrum obtained in $^{13}C_1$(4-phenol) tyrosinate. Note the line broadening of the spectrum due to the introduction of the nuclear spin. Ab initio calculations [68,71,72] and ^{17}O-labeling experiments by Babcock et al. [73] predict significant spin density at the phenolic oxygen of tyrosyl radical. There was no significant observed effect in the EPR spectrum due to ^{15}N labeling of the tyrosinate amino group (Fig. 6C).

While CW EPR spectroscopy detected no significant ^{15}N effect on tyrosyl radical, vibrational spectroscopy detected a ^{15}N shift, due to labeling of the tyrosinate amino group. In this experiment, FT-IR spectroscopy was coupled with flash photolysis to investigate the structural changes induced by the photolysis (oxidation) reaction. Spectra were recorded before and after photolysis (Fig. 7) and were then subtracted

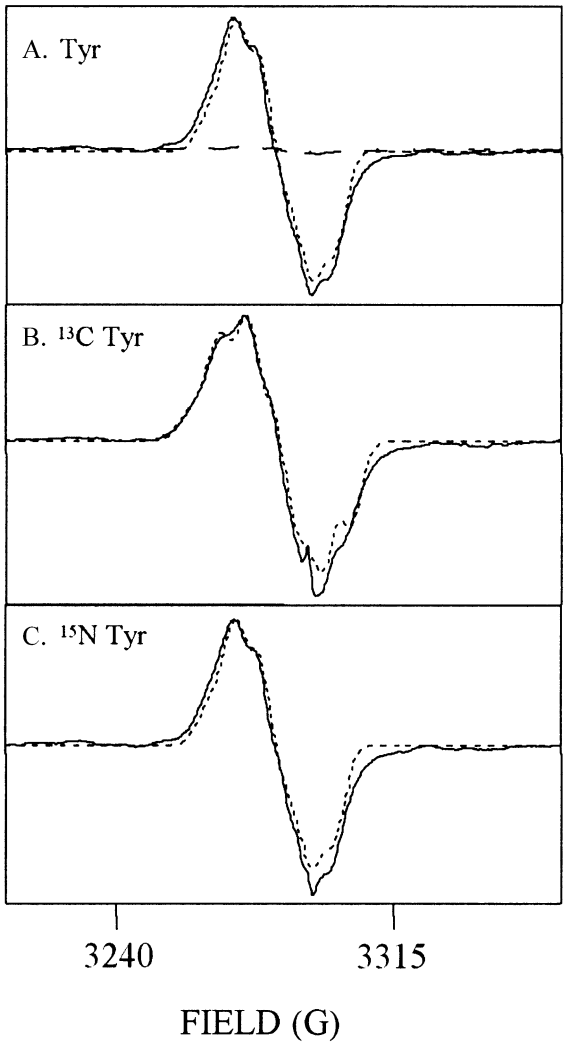

Fig. 6. EPR spectra of tyrosyl radical, produced by flash photolysis of tyrosinate, at 77 K. In A (solid line), natural abundance tyrosinate was employed. The dashed line in A shows the result of photolysis on the borate buffer. In B (solid line), $^{13}C_1$ labeled (at the ring carbon 4) tyrosinate was employed. In C (solid line), ^{15}N tyrosinate was employed. In each panel, the superimposed, dotted line shows the result of spectral simulation. EPR simulations were performed through the use of a computer program written by Hoganson and Babcock [76]. Hyperfine interactions were obtained from Ref. [70] with minor modifications [68]. The g value was obtained experimentally, and the g tensor was: $g_{xx}=2.0070$, $g_{yy}=2.0046$, $g_{zz}=2.0024$. The linewidth was 2.7, and the frequency = 9.21 GHz. (Figure reprinted with permission from Ref. [68]. Copyright (2002) *Journal of the American Chemical Society.*)

to give the oxidation spectrum [67,68]. The expected changes are perturbations to the ring stretching and CO stretching vibrations, as unpaired spin density delocalizes to the phenol oxygen [45,46]. Bands in the FT-IR difference spectrum (Fig. 7A) were indeed assignable to ring and CO stretching vibrational modes [68]. For example, bands were observed to be sensitive to ^{13}C labeling of the aromatic ring. However, the observation that ^{15}N labeling causes shifts of vibrational bands in the difference spectrum was unexpected (Fig. 7B,C). We attributed these isotopic shifts to in plane bending modes of the amino group (Fig. 1A). To contribute to the difference spectrum, the amino group must be perturbed by the oxidation of the aromatic ring [68].

One possible explanation for the oxidation-induced perturbation of the amino group is a small amount of spin density migration from the aromatic ring to the amino group. Other possible explanations have been discussed [68]. Such a spin density migration has been predicted to occur in tryptophan cation radicals, on the basis of ab initio calculations [74]. Our density functional calculations on tyrosyl radical, performed in collaboration with Prof. Darrin York and Kevin Range at the University of Minnesota, also predicted that such spin density migration can occur [68]. These calculations are in agreement with work of Wheeler et al. [71], but do not agree with the conclusions of [75]. However, in [75] only one vibrational band was considered with an arbitrary scaling factor. The calculations of York and Range also indicated that the in plane bending vibration of the amino group will be altered in frequency (Range et al., unpublished results), due to spin delocalization. From these calculations, the magnitude of the putative, nitrogen hyperfine coupling was calculated as less than 0.5 G. As shown by simulations with and without the ^{15}N coupling, such a small hyperfine coupling to nitrogen would not be detectable in our CW EPR experiments. However, this small delocalization of spin is detectable by vibrational spectroscopy.

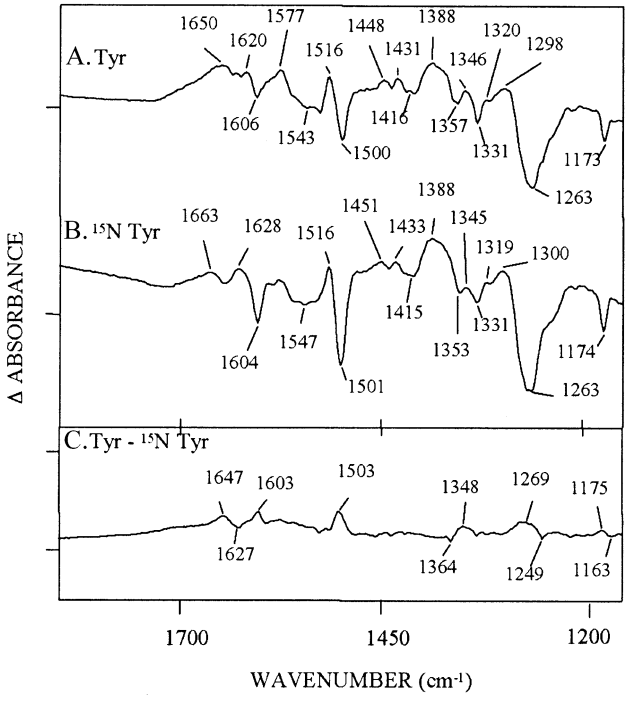

Fig. 7. Difference FT-IR spectra, associated with the oxidation of tyrosinate by flash photolysis, at 77 K. In A, natural abundance tyrosinate was employed. In B, ^{15}N-labeled tyrosinate was employed. The double-difference spectrum (A-minus-B) is shown in C. (Figure reprinted with permission from Ref. [68]. Copyright (2002) *Journal of the American Chemical Society.*)

10. Oxidation of tyrosinate in tyrosine-containing dipeptides

A reasonable extrapolation of these conclusions is that spin density delocalization to the amide nitrogen can occur when tyrosyl radicals are formed in peptides and proteins. The idea that spin density may move into the amide bond is important because it implies that electron transfer may be mediated through the peptide backbone in redox-active tyrosine containing proteins. To test the idea that spin density may delocalize into the amide bond, we performed flash photolysis studies with tyrosine-containing dipeptides [68]. In PSII, tyrosine Z and D are contained in the highly conserved sequence, Ile-Tyr-Pro [3]. Accordingly, we investigated two sets of dipeptides, one that contains Tyr on the amino terminus and one that contains Tyr on the carboxyl terminus (Fig. 1B). Data on Ile/Tyr and Pro/Tyr peptides are discussed here. In all four cases, an EPR signal was produced that is characteristic of tyrosyl radical [68]. In the Tyr-Pro case, a small perturbation was observed, consistent with a small change in methylene angle. The FT-IR absorption spectrum showed changes relative to the tyrosinate spectrum, consistent with the formation of the amide or imide bond and with spectral contributions from the additional amino acid side chain [68]. Interestingly, the photolysis-induced FT-IR spectrum of the dipeptide showed perturbations, relative to the photolysis spectrum of tyrosinate. In particular, potential amide and imide contributions were observed in the photolysis spectrum (Fig. 8, solid fill). Note that sequence-dependent changes in the frequency of the CC tyrosine ring stretching and CO tyrosine stretching vibrations [68] were also observed (Fig. 8). These sequence-dependent changes may be due to alterations in conformation. One interpretation of this result is that spin density delocalization occurs both in tyrosinate and in tyrosinate-containing dipeptides [68].

11. Implications for redox-active tyrosines in PSII and other enzymes

Our experiments on dipeptides imply that spin delocalization may be important in proteins and enzymes, which use redox-active tyrosines as electron transfer intermediaries. Based on this hypothesis, some predictions can be made. First, this idea predicts significant couplings to the amide N in tyrosine D and Z, which might be detectable by ESEEM or pulsed EPR techniques. Actually, indirect evidence for such a coupling in D^{ox} has been already published in a study in which ^{15}N histidine and ^{15}N global labeling were employed [36]. Second, we would expect that the FT-IR spectrum associated with tyrosinate oxidation in proteins would differ in some respects from the oxidation spectrum of tyrosinate in vitro. In particular, downshifts of the CO stretching frequency might be observed, as spin density delocalizes into the peptide bond. Downshifts of the tyrosyl radical CO vibration were observed in some tyrosine-containing dipeptides [68], and a substantial downshift of the CO vibration has been described previously for the tyrosyl radical in ribonucleotide reductase [69]. In addition, our work has suggested that the CO frequencies of Z^{ox} and D^{ox} are downshifted from the CO frequency observed in tyrosinate [19,47,48,50,54,55,63]. Third, the hypothesis predicts that there will be amide and imide contributions to difference FT-IR spectrum, associated with tyrosine D and Z photooxidation. Evidence for amide I and II contributions to

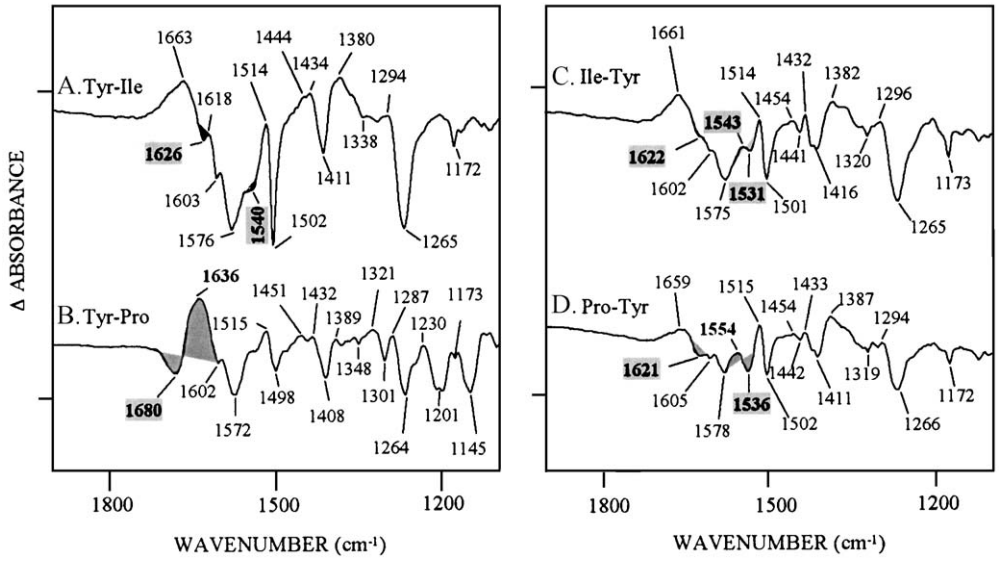

Fig. 8. Difference FT-IR spectra, associated with the oxidation of tyrosinate in dipeptides. The radical was generated by flash photolysis at 77 K. The dipeptides had the sequence, tyr–ile (A), tyr–pro (B), ile–tyr (C), and pro–tyr (D). (Figure reprinted with permission from Ref. [68]. Copyright (2002) *Journal of the American Chemical Society.*)

these FT-IR spectra has been obtained with ^{15}N labeling [48] and by comparison to model compounds [63].

It will be interesting to examine other tyrosyl radical containing enzymes to see if these are general phenomena. Little is known about how the protein environment controls the energetics and kinetics of redox-active tyrosines. The idea that spin density may move into the amide bond is important because it implies that electron transfer may be mediated through the peptide backbone in redox-active tyrosine-containing proteins. Such sequence-dependent spin delocalization from the aromatic ring into the amide bond provides a possible mechanism for directional and midpoint potential control in some redox-active tyrosines.

Acknowledgements

We thank all members of the Barry laboratory, past and present. In particular, we are grateful to those Barry group members, who have investigated the structure and function of tyrosyl radicals, including Dr. Renee Boerner, Prof. Gina MacDonald, Mr. George Noren, Dr. Chenglie Ma, Prof. Sunyoung Kim, Dr. Reza Razeghifard, Dr. Kathryn Bixby, Ms. Enid González, and Dr. Mary Bernard. We are grateful to Mr. Thomas Krick at the University of Minnesota Mass Spectrometry Center and to all our tyrosyl radical collaborators, including Prof. Darrin York (UM), Mr. Kevin Range (UM), and Prof. Ólöf Einarsdóttir (UC Santa Cruz). We also thank Prof. R. Wheeler (University of Oklahoma) for collaborative efforts on the plastoquinone vibrational spectrum and for many helpful discussions. B.A.B. offers this paper in tribute to the scientific career of G.T. Babcock.

This work was supported by NIH GM43273 (B.A.B.) and GM19541 (I. P.-A).

References

[1] R.D. Britt, Oxygen evolution, in: D.R. Ort, C.F. Yocum (Eds.), Oxygenic Photosynthesis: The Light Reactions, vol. 4. Kluwer Academic Publishing, Dordrecht, 1996, pp. 137–164.

[2] G.M. Ananyev, I. Sakiyan, B.A. Diner, G.C. Dismukes, A functional role for tyrosine-D in assembly of the inorganic core of the water complex of photosystem II and the kinetics of water oxidation, Biochemistry 41 (2002) 974–980.

[3] B.A. Barry, R.J. Boerner, J.C. de Paula, The use of cyanobacteria in the study of the structure and function of photosystem II, in: D. Bryant (Ed.), The Molecular Biology of the Cyanobacteria, vol. 1. Kluwer Academic Publishing, Dordrecht, 1994, pp. 215–257.

[4] O. Nanba, K. Satoh, Isolation of a photosystem II reaction center consisting of D-1 and D-2 polypeptides and cytochrome *b*-559, Proc. Natl. Acad. Sci. U. S. A. 84 (1987) 109–112.

[5] A. Zouni, H.-T. Witt, J. Kern, P. Fromme, N. Krauß, W. Saenger, P. Orth, Crystal structure of photosystem II from *Synechoccus elongatus* at 3.8 Å resolution, Nature 409 (2001) 739–743.

[6] N. Kamiya, J.-R. Shen, Crystal structure of oxygen-evolving photosystem II from *Thermosynechococcus vulcanus* at 3.7 A resolution, Proc. Natl. Acad. Sci. U. S. A. 100 (2003) 98–103.

[7] S. Gerken, K. Brettel, E. Schlodder, H.T. Witt, Optical characterization of the immediate donor to Chlorophyll a_{II}^{+} in O_2-evolving photosystem II complexes, FEBS Lett. 237 (1988) 69–75.

[8] R.J. Debus, B.A. Barry, G.T. Babcock, L. McIntosh, Site-specific mutagenesis identifies a tyrosine radical involved in the photosynthetic oxygen-evolving complex, Proc. Natl. Acad. Sci. U. S. A. 85 (1988) 427–430.

[9] W.F.J. Vermaas, A.W. Rutherford, Ö. Hansson, Site-directed mutagenesis in photosystem II of the cyanobacterium *Synechocystis* sp. PCC 6803: donor D is a tyrosine residue in the D2 protein, Proc. Natl. Acad. Sci. U. S. A. 85 (1988) 8477–8481.

[10] R.J. Debus, B.A. Barry, I. Sithole, G.T. Babcock, L. McIntosh, Directed mutagenesis indicates that the donor to P680+ in photosystem II is Tyr-161 of the D1 polypeptide, Biochemistry 27 (1988) 9071–9074.

[11] J.G. Metz, P.J. Nixon, M. Rögner, G.W. Brudvig, B.A. Diner, Directed alteration of the D1 polypeptide of photosystem II: evidence that tyrosine-161 is the redox component, Z, connecting the oxygen-evolving complex to the primary electron donor P680, Biochemistry 28 (1989) 6960–6969.

[12] G.H. Noren, B.A. Barry, The YF161D1 mutant of *Synechocystis* 6803 exhibits an EPR signal from a light-induced photosystem II radical, Biochemistry 31 (1992) 3335–3342.

[13] J. Deisenhofer, H. Michel, The photosynthetic reaction center from the purple bacterium *Rhodopseudomonas viridis*, Science 245 (1989) 1463–1473.

[14] A. Boussac, A.L. Etienne, Midpoint potential of Signal II (Slow) in Tris-washed photosystem-II particles, Biochim. Biophys. Acta 766 (1984) 576–581.

[15] J.P. Dekker, J.J. Plijter, L. Ouwehand, H.J. van Gorkom, Kinetics of manganese redox transitions in the oxygen-evolving apparatus of photosynthesis, Biochim. Biophys. Acta 767 (1984) 176–179.

[16] G.T. Babcock, R.E. Blankenship, K. Sauer, Reaction kinetics for positive charge accumulation on the water side of chloroplast Photosystem II, FEBS Lett. 61 (1976) 286–289.

[17] M. Boska, K. Sauer, Kinetics of EPR Signal IIvf in chloroplast Photosystem II, Biochim. Biophys. Acta 765 (1984) 84–87.

[18] I. Pujols-Ayala, B.A. Barry, His 190-D1 and Glu 189-D1 provide structural stabilization in photosystem II, Biochemistry 41 (2002) 11456–11465.

[19] S. Kim, I. Ayala, J.J. Steenhuis, E.T. Gonzalez, M.R. Razeghifard, B.A. Barry, Infrared spectroscopic identification of the C–O stretching vibration associated with the tyrosyl Z• and D• radicals in photosystem II, Biochim. Biophys. Acta 1366 (1998) 330–354.

[20] B.A. Barry, Tyrosyl radicals in Photosystem II, Methods Enzymol. 258 (1995) 303–319.

[21] R.J. Boerner, B.A. Barry, Isotopic labeling and EPR spectroscopy show that a tyrosine residue is the terminal electron donor, Z, in manganese-depleted photosystem II preparations, J. Biol. Chem. 268 (1993) 17151–17154.

[22] K. Warnke, G.T. Babcock, J. McCracken, Structure of the Y_D tyrosine radical in photosystem II as revealed by ^2H electron spin echo envelope modulation (ESEEM) spectroscopic analysis of hydrogen hyperfine interactions, J. Am. Chem. Soc. 116 (1994) 7332–7340.

[23] C. Tommos, X.-S. Tang, K. Warncke, C.W. Hoganson, S. Styring, J. McCracken, B.A. Diner, G.T. Babcock, Spin-density distribution, conformation, and hydrogen bonding of the redox-active tyrosine Yz in photosystem II from multiple electron magnetic resonance spectroscopies: implications for photosynthetic oxygen evolution, J. Am. Chem. Soc. 117 (1995) 10325–10335.

[24] X.S. Tang, M. Zheng, D.A. Chisholm, G.C. Dismukes, B.A. Diner, Investigation of the differences in the local protein environments surrounding tyrosine radicals YZ and YD in photosystem II using wild-type and the D2-Tyr160Phe mutant of *Synechocystis* 6803, Biochemistry 35 (1996) 1475–1484.

[25] B.A. Diner, D.A. Force, D.W. Randall, R.D. Britt, Hydrogen bonding, solvent exchange, and coupled proton and electron transfer in the oxidation and reduction of redox-active tyrosine Y-z in Mn-depleted core complexes of Photosystem II, Biochemistry 37 (1998) 17931–17943.

[26] B.A. Barry, G.T. Babcock, Tyrosine radicals are involved in the photosynthetic oxygen-evolving system, Proc. Natl. Acad. Sci. U. S. A. 84 (1987) 7099–7103.
[27] S. Kim, J. Liang, B.A. Barry, Chemical complementation identifies a proton acceptor for redox-active tyrosine D in photosystem II, Proc. Natl. Acad. Sci. U. S. A. 94 (1997) 14406–14412.
[28] H. Kühne, G.W. Brudvig, Proton-coupled electron transfer involving tyrosine Z in Photosystem II, J. Phys. Chem., B 106 (2002) 8189–8196.
[29] P. Faller, R.J. Debus, K. Brettel, M. Sugiura, A.W. Rutherford, A. Boussac, Rapid formation of the stable tyrosyl radical in photosystem II, Proc. Nat. Acad. Sci. U. S. A. 98 (2001) 14368–14373.
[30] P. Faller, A.W. Rutherford, R.J. Debus, Tyrosine D oxidation at cryogenic temperature in photosystem II, Biochemistry 41 (2002) 12914–12920.
[31] B. Svensson, I. Vass, E. Cedergren, S. Styring, Structure of donor side components in photosystem II predicted by computer modelling, EMBO 7 (1990) 2051–2059.
[32] S.V. Ruffle, D. Donnelly, T.L. Blundell, J.H.A. Nugent, A three-dimensional model of the photosystem II reaction centre of *Pisum sativum*, Photosynth. Res. 34 (1992) 287–300.
[33] X.-S. Tang, D.A. Chisholm, G.C. Dismukes, G.W. Brudvig, B.A. Diner, Spectroscopic evidence from site-directed mutants of *Synechocystis* PCC6803 in favor of a close interaction between histidine 189 and redox-active tyrosine 160, both of the polypeptide D2 of the photosystem II reaction center, Biochemistry 32 (1993) 13742–13748.
[34] C. Tommos, L. Davidsson, B. Svensson, C. Madsen, W. Vermaas, S. Styring, Modified EPR spectra of the tyrosine$_D$ radical in photosystem II in site-directed mutants of *Synechocystis* sp. PCC 6803: identification of side chains in the immediate vicinity of tyrosine$_D$ on the D2 protein, Biochemistry 32 (1993) 5436–5441.
[35] S. Un, X.-S. Tang, B.A. Diner, 245 GHz high-field EPR study of tyrosine-D^o and tyrosine-Z^o in mutants of photosystem II, Biochemistry 35 (1996) 679–684.
[36] K.A. Campbell, J.M. Peloquin, B.A. Diner, X.-S. Tang, D.A. Chisholm, R.D. Britt, The τ-Nitrogen of D2 histidine 189 is the hydrogen bond donor to the tyrosine radical YD• of photosystem II, J. Am. Chem. Soc. 119 (1997) 4787–4788.
[37] R.A. Roffey, K.-J. van Wijk, R.T. Sayre, S. Styring, Spectroscopic characterization of Tyr$_Z$ in histidine 190 mutants of the D1-protein in photosystem II in *Chlamydomonas reinhardtii*: implications for the structural model of the donor side of PSII, J. Biol. Chem. 269 (1994) 5115–5121.
[38] M.T. Bernard, G.M. MacDonald, A.P. Nguyen, R.J. Debus, B.A. Barry, A difference infrared study of hydrogen bonding to the Z• tyrosyl radical of photosystem II, J. Biol. Chem. 270 (1995) 1589–1594.
[39] A.-M.A. Hays, I.R. Vassiliev, J.H. Golbeck, R.J. Debus, Role of D1-His190 in proton-coupled electron transfer reactions in photosystem II: a chemical complementation study, Biochemistry 37 (1998) 11352–11365.
[40] F. Mamedov, R.T. Sayre, S. Styring, Involvement of histidine 190 on the D1 protein in electron/proton transfer reactions on the donor side of Photosystem II, Biochemistry 37 (1998) 14245–14256.
[41] A. Zouni, J. Kern, B. Loll, P. Fromme, P. Orth, N. Krauss, W. Saenger, J. Biesiadka, Biochemical characterization and crystal structure of water oxidizing Photosystem II from *Synechoccus elongatus*, in: U. Luttge, B. Osmond, R. Voesenek (Eds.), Proceedings of the 12th International Congress on Photosynthesis, Thieme, Stuttgart, 2002, pp. S05–003.
[42] P.J. O'Malley, G.T. Babcock, R.C. Prince, The cationic plastoquinone radical of the chloroplast water splitting complex: hyperfine splitting from a single methyl group determines the EPR spectral shape of Signal II, Biochim. Biophys. Acta 766 (1984) 283–288.
[43] B.A. Barry, M.K. El-Deeb, P.O. Sandusky, G.T. Babcock, Tyrosine radicals in photosystem II and related model compounds, J. Biol. Chem. 265 (1990) 20139–20143.
[44] G.H. Noren, R.J. Boerner, B.A. Barry, EPR characterization of an oxygen-evolving photosystem II preparation from the cyanobacterium *Synechocystis* 6803, Biochemistry 30 (1991) 3943–3950.
[45] G.N.R. Tripathi, R.H. Schuler, The resonance Raman spectrum of phenoxyl radical, J. Chem. Phys. 81 (1984) 113–121.
[46] C.R. Johnson, M. Ludwig, S.A. Asher, Ultraviolet resonance Raman characterization of photochemical transients of phenol, tyrosine, and tryptophan, J. Am. Chem. Soc. 108 (1986) 905–912.
[47] G.M. MacDonald, K.A. Bixby, B.A. Barry, A difference FT-IR study of two redox-active tyrosine residues in photosystem II, Proc. Natl. Acad. Sci. U. S. A. 90 (1993) 11024–11028.
[48] S. Kim, B.A. Barry, The protein environment surrounding tyrosyl radicals D• and Z• in photosystem II: a difference FT-IR study, Biophys. J. 74 (1998) 2588–2600.
[49] M.R. Razeghifard, S. Kim, J.S. Patzlaff, R.S. Hutchison, T. Krick, I. Ayala, J.J. Steenhuis, S.E. Boesch, R.A. Wheeler, B.A. Barry, The in vivo, in vitro, and calculated vibrational spectra of plastoquinone and the plastosemiquinone anion radical, J. Phys. Chem. B103 (1999) 9790–9800.
[50] S. Kim, J. Patzlaff, T. Krick, I. Ayala, R.K. Sachs, B.A. Barry, Isotope-based discrimination between the infrared modes of plastosemiquinone anion radicals and neutral tyrosyl radicals in photosystem II, J. Phys. Chem., B 104 (2000) 9720–9727.
[51] R. Hienerwadel, A. Boussac, J. Breton, B.A. Diner, C. Berthomieu, Fourier transform infrared difference spectroscopy of photosystem II tyrosine D using site-directed mutagenesis and specific isotope labeling, Biochemistry 36 (1997) 14712–14723.
[52] T. Noguchi, Y. Inoue, X.-S. Tang, Structural coupling between the oxygen-evolving Mn cluster and a tyrosine residue in photosystem II as revealed by Fourier transform infrared spectroscopy, Biochemistry 36 (1997) 14705–14711.
[53] C. Berthomieu, R. Hienerwadel, A. Boussac, J. Breton, B.A. Diner, Hydrogen bonding of redox-active tyrosine Z in photosystem II probed by FTIR difference spectroscopy, Biochemistry 37 (1998) 10547–10554.
[54] S. Kim, B.A. Barry, The vibrational spectrum associated with the reduction of tyrosyl radical, D•: a comparative biochemical and kinetic study, Biochemistry 37 (1998) 13882–13892.
[55] I. Ayala, S. Kim, B.A. Barry, A difference Fourier transform infrared study of tyrosyl radical Z• decay in photosystem II, Biophys. J. 77 (1999) 2137–2144.
[56] C. Berthomieu, E. Nabedryk, W. Mäntele, J. Breton, Characterization by FTIR spectroscopy of the photoreduction of the primary quinone acceptor Q_A in photosystem II, FEBS Lett. 269 (1990) 363–367.
[57] H. Zhang, M.R. Razeghifard, G. Fischer, T. Wydrzynski, A time-resolved FTIR difference study of the plastoquinone Q_A and redox-active tyrosine Y_Z interactions in photosystem II, Biochemistry 36 (1997) 11762–11768.
[58] H. Zhang, G. Fischer, T. Wydrzynski, Room-temperature vibrational difference spectrum for $S_2Q_B^-/S_1Q_B$ of photosystem II determined by time-resolved Fourier transform infrared spectroscopy, Biochemistry 37 (1998) 5511–5517.
[59] G.M. MacDonald, J.J. Steenhuis, B.A. Barry, A difference infrared spectroscopic study of chlorophyll oxidation in hydroxylamine treated photosystem II, J. Biol. Chem. 270 (1995) 8420–8428.
[60] A. Cua, D.H. Stewart, G.W. Brudvig, D.F. Bocian, Selective resonance Raman scattering from chlorophyll Z in photosystem II via excitation into the near-infrared absorption band of the cation, J. Am. Chem. Soc. 120 (1998) 4532–4533.
[61] G.M. MacDonald, B.A. Barry, Difference FT-IR study of a novel biochemical preparation of photosystem II, Biochemistry 31 (1992) 9848–9856.
[62] D.F. Ghanotakis, G.T. Babcock, Hydroxylamine as an inhibitor between Z and P_{680} in Photosystem II, FEBS Lett. 153 (1983) 231–234.

[63] I. Pujols-Ayala, C.A. Sacksteder, B.A. Barry, Redox-active tyrosine residues: role for the peptide bond in electron transfer, J. Am. Chem. Soc. 125 (2003) 7536–7538.
[64] H. Takeuchi, N. Watanabe, Y. Satoh, I. Harada, Effects of hydrogen bonding on the tyrosine Raman bands in the 1300–1150 cm^{-1} region, J. Raman Spectrosc. 20 (1989) 233–237.
[65] R.S. Hutchison, J.J. Steenhuis, C.F. Yocum, R.M. Razeghifard, B.A. Barry, Deprotonation of the 33 kDa, extrinsic, manganese stabilizing protein accompanies photooxidation of manganese in photosystem II, J. Biol. Chem. 274 (1999) 31987–31995.
[66] C. Berthomieu, C. Boullais, J.M. Neumann, A. Boussac, Effect of C-13, O-18, and H-2-labeling on the infrared modes of UV-induced phenoxyl radicals, Biochim. Biophys. Acta 1365 (1998) 112–116.
[67] J.A. Cappuccio, I. Ayala, G.I. Elliot, I. Szundi, J. Lewis, J.P. Konopelski, B.A. Barry, O. Einarsdottir, Modeling the active site of cytochrome oxidase: synthesis and characterization of a cross-linked histidine–phenol, J. Am. Chem. Soc. 124 (2002) 1750–1760.
[68] I. Ayala, K. Range, D. York, B.A. Barry, Spectroscopic properties of tyrosyl radicals in dipeptides, J. Am. Chem. Soc. 124 (2002) 5496–5505.
[69] G. Backes, M. Sahlin, B.M. Sjoeberg, T.M. Loehr, J. Sanders-Loehr, Resonance Raman spectroscopy of ribonucleotide reductase. Evidence for a deprotonated tyrosyl radical and photochemistry of the binuclear iron center, Biochemistry 28 (1989) 1923–1929.
[70] R.J. Hulsebosch, J.S. van der Brink, S.A.M. Niewenhuis, P. Gast, J. Raap, J. Lugtenburg, A.J. Hoff, Electronic structure of the neutral tyrosine radical in frozen solution. Selective ^{2}H-, ^{13}C-, and ^{17}O-isotope labeling and EPR spectroscopy at 9 and 35 GHz, J. Am. Chem. Soc. 119 (1997) 8685–8694.
[71] Y. Qin, R.A. Wheeler, Similarities and differences between phenoxyl and tyrosine phenoxyl radical structures, vibrational frequencies, and spin densities, J. Am. Chem. Soc. 117 (1995) 6083–6092.
[72] F. Himo, A. Graslund, L.A. Eriksson, Density functional calculations on model tyrosyl radicals, Biophys. J. 72 (1997) 1556–1567.
[73] F. Dole, B.A. Diner, C.W. Hoganson, G.T. Babcock, R.D. Britt, Determination of the electron spin density on the phenolic oxygen of the tyrosyl radical of photosystem II, J. Am. Chem. Soc. 119 (1997) 11540–11541.
[74] S.E. Walden, R.A. Wheeler, First evidence of anchimeric spin delocalization in tryptophan radical cation, J. Am. Chem. Soc. 119 (1997) 3175–3176.
[75] P.J. O'Malley, Density functional calculations modelling tyrosine oxidation in oxygenic photosynthetic electron transfer, Biochim. Biophys. Acta 1553 (2002) 212–217.
[76] C.W. Hoganson, G.T. Babcock, Protein–tyrosyl radical interactions in photosystem II studied by electron spin resonance and electron nuclear double resonance spectroscopy: comparison with ribonucleotide reductase and in vitro tyrosine, Biochemistry 31 (1992) 11874–11880.
[77] K.N. Ferreira, T.M. Ivenson, K. Maghlaoui, J. Barber, S. Iwata, Architecture of Photosynthetic oxygen-evolving center, Science, (2004) (in press).